Electrostatic Interactions

DOI: 10.1002/ange.200502586

Designing Intermolecular Interactions between Halogenated Peripheries of Inorganic and Organic Molecules: Electrostatically Directed M–X···X′–C Halogen Bonds**

Guillermo Mínguez Espallargas, Lee Brammer, and Paul Sherwood*

Halogen atoms (X) typically form a covalent single bond to only one other atom within a molecule, which places them most frequently at the periphery of that molecule and, thus, at molecular interfaces in condensed phases. Such terminally

[*] G. Mínguez Espallargas, Dr. L. Brammer
Department of Chemistry
University of Sheffield
Sheffield S3 7HF (UK)
Fax: (+44) 114-222-9346
E-mail: lee.brammer@sheffield.ac.uk
Dr. P. Sherwood
Computational Science and Engineering Department
CCLRC Daresbury Laboratory
Daresbury, Warrington WA4 4AD (UK)

[**] This work was supported by the Cambridge Crystallographic Data Centre and the CCLRC Centre for Molecular Structure and Dynamics. We thank Stephen L. Purver and Harry Adams (University of Sheffield) for initial work on compound **1** and its crystal structure.

Supporting information for this article is available on the WWW under http://www.angewandte.org or from the author.

bonded halogen atoms, while not bordering on ubiquity like hydrogen atoms, are nevertheless abundant and found in a wide range of organic and inorganic molecules.[1] Thus, the development of reliable intermolecular interactions that involve such halogen atoms has the potential for widespread application in supramolecular chemistry and crystal engineering. We have pursued such a design and recently reported the application of directional M–Cl···X–C nucleophile–electrophile interactions in the synthesis of both neutral[2] and ionic molecular crystals.[3]

The basis for the design of these interactions was the known behavior in intermolecular interactions of inorganic halogen species (M–X) as directional Lewis bases and of organic halogen species (C–X) as directional Lewis acids. Specifically metal–halide groups (M–X) have been shown to be potent and directional hydrogen-bond acceptors,[4] with applications in crystal design and synthesis.[5] Organic halogen species (C–X), particularly for X = I, Br, and Cl, form halogen bonds[6] most commonly with organic bases, for example, N/O···X–C,[7] but potentially also with other halogen atoms.[8] Halogen bonds have been applied to various aspects of supramolecular assembly in the solid state.[6,9] However, although the nature of hydrogen bonds that involve inorganic halogen species is quite well established, in line with that of other strong hydrogen bonds, the nature of halogen bonds that involve organic halogen species is not fully established. Indeed, at the weakest end of the scale of interaction energies, interactions between chlorocarbon groups C–Cl···Cl–C, which are directional in the solid state, have been the subject of dispute in regard to whether they are weakly attractive[10] or guided by adopting the least-repulsive interaction geo metry.[11] Halogen bonds are often discussed in terms of a charge transfer between the Lewis base and the C–X σ* orbital,[6] by analogy to halogen bonds that involve dihalogen molecules, for example, N···X–X,[12] or most emphatically I^-···I–I, which gives rise to the symmetrical I_3^- molecular ion and much related polyiodide network chemistry.[13] However, our most recent study of M–Cl···X–C networks in crystals of the compounds *trans*-[MCl_2(3-Xpy)$_2$] (M = Pt, Pd; 3-Xpy = 3-halopyridine; X = I, Br, Cl, F) shows that the absence of M–Cl···F-C interactions, the apparent relative interaction strengths (I > Br > Cl) and the prevalent interaction geometry (approximately linear Cl···X–C and markedly bent M–Cl···X interactions) are all consistent with the relative magnitude and anisotropic nature of the electrostatic potential around the inorganic and organic halogen species.[2] Thus, an electrostatic component to M–X···X′–C interactions may be quite important, although the use of only one type of halide ligand and the adoption of five separate propagated networks with M–Cl···X–C interactions limited the extent to which the importance of the electrostatic contribution could be assessed relative to other contributors, notably charge transfer.

The present study overcomes these difficulties by examining a series of eight isostructural compounds in which both the organic and inorganic halogen species have been varied in a systematic manner: (4-X′pyH)$_2$[CoX_4] (4-X′pyH = 4-halopyridinium; **1**: X′ = Cl, X = Cl; **2**: X′ = Br, X = Cl; **3**: X′ = Cl, [CoX_4] = $CoCl_{1.56}Br_{2.44}$; **4**: X′ = Br, [CoX_4] = $CoCl_{1.62}Br_{2.38}$; **5**: X′ = Cl, X = Br; **6**: X′ = Br, X = Br; **7**: X′ = Cl, X = I; **8**: X′ = Br, X = I). This series of compounds provides a unique opportunity to assess the relative importance of the charge-transfer and electrostatic contributions to the M–X···X′–C halogen bonds through consideration of the structural changes imparted by changing either the organic or the inorganic halogen species. Compounds **3** and **4** further allow interpolation between the discrete steps afforded by changing all the organic or inorganic halogen species. Theoretical calculations have been used to understand the structural changes that arise across the series through examination of the changes in electrostatic potential and to understand the unusually large distortion from the tetrahedral geometry of the anions that has been observed across all of the crystal structures.

The crystal structures of **1**–**8**, determined at 150 K, show that each forms networks propagated by N–H···X_2Co hydrogen bonds and Co–X···X′–C halogen bonds (Figure 1). Pairs

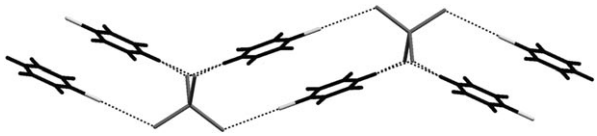

Figure 1. Network formed in crystal structures of **1**–**8**. Cobalt and halide ligands shown in dark gray, organic halogen atoms in light gray, and all other atoms in black (C, H, N).

of cations link each anion to its neighbor in the zigzag chain, with the cations adopting a stacked arrangement with mutually opposed molecular dipoles. The interaction geometries are summarized in Table 1. Notably the anions exhibit a large distortion (approximately C_{2v}) from the idealized tetrahedral geometry wherein the angles between the pairs of halide ligands that participate in hydrogen bonding are markedly decreased in magnitude (average Cl-Co-Cl: 98.0°; Br-Co-Br: 99.6°; I-Co-I: 102.4°) whereas the pairs of halide ligands involved in halogen bonding exhibit slightly enlarged angles (average Cl-Co-Cl: 110.9°; Br-Co-Br: 111.5°; I-Co-I: 112.4°).

The N–H···X_2Co bifurcated hydrogen bonds are asymmetric, as is common for tetrahedral halometallate anions,[5a] and become weaker and more symmetric on going from chloride to iodide ligands. Interestingly the hydrogen bonds are systematically more symmetric for the chloropyridinium cations than for the bromopyridinium cations when pairs of compounds that contain the same anion are compared.

Most interesting, however, are the Co–X···X′–C halogen bonds. All exhibit approximately linear geometries at the organic halogen atom (C–X′···X: 168.6–174.9°), whereas the Co–X···X′ angle is markedly bent (range: 120.3–123.7°), which confirms the nucleophilic–electrophilic nature of these interactions and, thus, the distinct roles of the two halogen atoms. Using the halogen–halogen distance measure $R_{XX'}$, normalized to account for differences in the van der Waals radii of the different halogen atoms,[7,15] it is clear that the halogen bonds are shorter, and by implication stronger, for the heavier organic halogen species (C–X), but weaker for

Table 1: Selected bond lengths, halogen bonds, and hydrogen-bond geometries for **1**–**8**.

	Co–X [Å]	C–X′ [Å]	X···X′ [Å] [$R_{XX'}$][a]	Co–X···X′ [°]	X···X′–C [°]	H···X[b] [Å] [R_{HX}][a]	N–H···X [°][b]
(4-ClpyH)$_2$[CoCl$_4$] (**1**)	2.2500(5)	1.723(2)	3.3428(6)	123.69(2)	173.75(7)	2.300 [0.78]	141.9
	2.2915(5)		[0.955]			2.825 [0.96]	134.0
(4-BrpyH)$_2$[CoCl$_4$] (**2**)	2.2532(9)	1.882(3)	3.2609(10)	121.61(4)	174.9(1)	2.249 [0.76]	146.0
	2.2842(10)		[0.906]			2.953 [1.00]	131.2
(4-ClpyH)$_2$[CoCl$_{1.56}$Br$_{2.44}$] (**3**)	2.3610(8)[c]	1.715(4)	3.4261(13)[c]	123.31(4)[c]	172.6(1)[c]	2.440[d] [0.81]	137.7[d]
	2.3586(9)[d]		[0.958][g]			2.831[d] [0.95]	136.6[d]
(4-BrpyH)$_2$[CoCl$_{1.62}$Br$_{2.38}$] (**4**)	2.3596(8)[e]	1.884(5)	3.3423(9)[e]	121.44(3)[e]	173.9(2)[e]	2.370[f] [0.79]	142.8[f]
	2.3477(10)[f]		[0.909][g]			2.968[f] [0.99]	133.5[f]
(4-ClpyH)$_2$[CoBr$_4$] (**5**)	2.3855(4)	1.718(3)	3.4898(8)	123.20(2)	171.1(1)	2.543 [0.83]	136.6
	2.4209(5)		[0.967]			2.854 [0.94]	137.1
(4-BrpyH)$_2$[CoBr$_4$] (**6**)	2.3859(9)	1.884(5)	3.3873(11)	121.23(3)	171.9(2)	2.478 [0.81]	140.6
	2.4162(10)		[0.915]			2.957 [0.97]	134.4
(4-ClpyH)$_2$[CoI$_4$] (**7**)	2.5820(7)	1.721(5)	3.7203(13)	121.70(3)	168.6(2)	2.877 [0.91]	132.1
	2.6021(7)		[0.997]			3.016 [0.95]	139.2
(4-BrpyH)$_2$[CoI$_4$] (**8**)	2.5806(7)	1.879(5)	3.6018(7)	120.26(3)	169.0(2)	2.811 [0.89]	135.0
	2.5994(8)		[0.940]			3.072 [0.97]	137.3

[a] $R_{XX'} = d(X\cdots X')/(r_X + r_{X'})$, where r_X and $r_{X'}$ are the van der Waals radii[14] of halogen atoms X and X′, respectively (following the definition of Lommerse et al.[7]); R_{HX} is defined analogously for the H···X separation. [b] Geometries calculated using hydrogen-atom positions normalized to standard nuclear positions, as established by neutron diffraction (N–H: 1.01 Å). [c] X = 78% Br, 22% Cl. [d] X = 44% Br, 56% Cl. [e] X = 76% Br, 24% Cl. [f] X = 43% Br, 57% Cl. [g] Arithmetic average.

the heavier inorganic halogen species (Co–X) (Table 1, Figure 2). The observed trend with respect to halogen bonds involving the Lewis acidic C–X group is consistent with

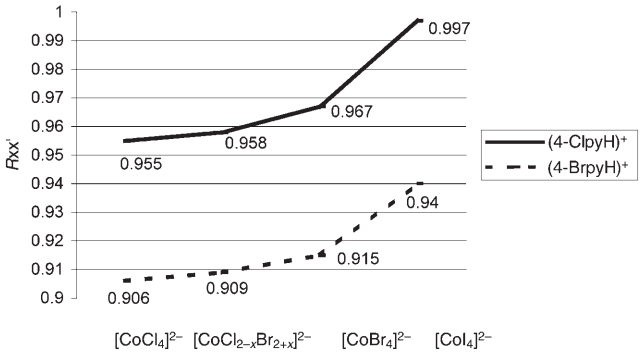

Figure 2. Variation of (Co)X···X′(C) halogen-bond lengths with change of the halogen atom. The distances $R_{XX'}$ are normalized as defined in Table 1 to account for differences in the van der Waals radii of the different halogen atoms.[7,15]

previous reports.[2,3,6–8] However, these results appear to be counter to the conventional wisdom that for halogen bonds involving halide ions (X^-) as the nucleophile, for example, $X^-\cdots$I–I (XI_2) or $X^-\cdots$Br–C, the halogen bonds are stronger or at least more prevalent for $I^- > Br^- > Cl^- > F^-$.[6,16] This prevailing view is based on a description of the halogen bonds as n→σ* charge-transfer interactions between the anion and the dihalogen or C–X group. Such an interaction is well established for trihalide ions and follows the presumed trend as evidenced by the geometries of the isostructural pairs $CsBrI_2/CsI_3$ and (RpyH)[ClI_2]/(RpyH)[BrI_2] (R = *N*-hexadecyl), wherein lengthening of the I–I bond occurs and this change is more pronounced for $I^- > Br^-$ and for $Br^- > Cl^-$, respectively.[17] Such a charge transfer would be less prominent for a C–X group as the σ* orbital will be higher in energy than for the corresponding I_2 molecule. Nevertheless, Resnati and co-workers have proposed that $I^-\cdots$Br–C halogen bonds are stronger than $Br^-\cdots$Br–C halogen bonds,[19] by inference from IR C–H stretching frequencies in *N*-methyl-3,5-dibromopyridinium halides, thus suggesting that n→σ* charge transfer is greater for the I^- ion, a better electron donor than the Br^- ion. One would, therefore, anticipate by analogy that the trend in decreasing $R_{XX'}$ distance, and thus increasing strength, would be X = Cl→Br→I if the n→σ* charge transfer were the dominant contributor to the halogen-bond strength for Co–X···X′–C in **1**–**8**. As the trend is the reverse (Figure 2), an alternative explanation must be sought.

As we have recently established that an electrostatic contribution is likely to be important in M–Cl···X–C halogen bonds,[2] we examined this possibility for M–X···X′–C halogen bonds in **1**–**8** through selected theoretical calculations. The electrostatic potential associated with the two cations and the three anions used has been calculated by using idealized geometries based upon those determined experimentally. All halogen atoms show an anisotropic potential that arises from their anisotropic charge distribution, with the most positive (or least negative) potential associated with the axial region *trans* to the covalent bond (M–X or C–X) and the most negative (or least positive) potential lying in an equatorial belt approximately orthogonal to the covalent bond (Figures 3 and 4). Distortion of the anion also leads to polarization and enhancement of the negative potential associated with the two halide ligands related by the smallest X-Co-X angle (compare the top of Figure 3a–c with the bottom of Figure 3d–f).

Anion–cation interactions involve the association of the most electropositive part of the cation, the N–H group, with the region of the most negative potential on the anion, located between the compressed pair of halide ligands. The Co–X···X′–C halogen bonds then bring together the most positive (axial) region of the organic halogen atoms with the region of greatest negative potential on the remaining inorganic

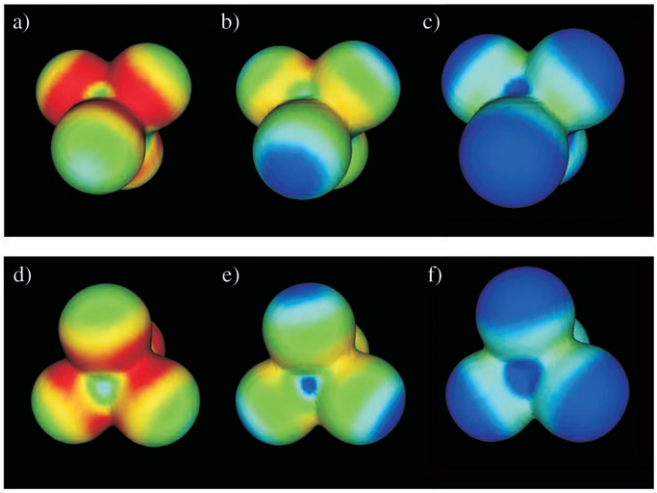

Figure 3. Calculated electrostatic potentials for the anions $[CoCl_4]^{2-}$ (a, d), $[CoBr_4]^{2-}$ (b, e), $[CoI_4]^{2-}$ (c, f); displayed on density isosurfaces of 0.0025 electrons bohr^{-3}, with a color range from red at 200 kcal mol^{-1} to blue at 160 kcal mol^{-1}. The views are approximately orthogonal to the twofold symmetry axes of the anions, with the halide ligands of the compressed CoX_2 moiety involved in hydrogen bonding at the top of the figures and those involved in halogen bonds at the bottom (cf. Scheme 1). The views (d–f) are rotated by 90° about the molecular twofold axes (vertical) relative to views (a–c).

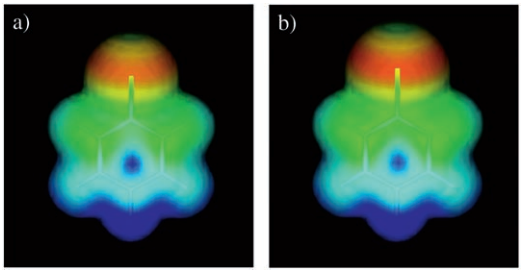

Figure 4. Calculated electrostatic potentials for the cations a) 4-chloropyridinium (4-ClpyH)$^+$ and b) 4-bromopyridinium (4-BrpyH)$^+$, displayed on density isosurfaces of 0.0025 electrons bohr^{-3}, with a color range from red at 70 kcal mol^{-1} to blue at 140 kcal mol^{-1}.

halogen atoms, thus resulting in near-linear X···X′–C angles and Co–X···X′ angles of approximately 120°.

The clear trend in the electrostatic potential across the three anions is a decrease in the magnitude of the negative potential on the corresponding density isosurfaces in the sequence $[CoCl_4]^{2-} > [CoBr_4]^{2-} > [CoI_4]^{2-}$ (Figure 3 a–c or d–f), which correlates with the trend of increasing halogen bonds lengths ($R_{ClX} < R_{BrX} < R_{IX}$; see Table 1). In addition, the positive potential along the C–X axis of the organic halogen species decreases from Br to Cl (Figure 4) in parallel with the trend $R_{XBr} < R_{XCl}$. These correlations taken together with the observed X···X′–C and Co–X···X′ angles are clearly consistent with the Co–X···X′–C halogen bonds being governed by a directional electrostatic interaction. The discrimination between the hydrogen bonding and halogen-bonding sites on the anions is also emphasized by the observation that in the structures of **3** and **4**, the two halide sites with a high chloride content are involved in hydrogen-bond formation whereas the two with a lower chloride content form the halogen bonds.[20]

Finally, we also determined the likely cause of the unusually large distortion from the idealized tetrahedral geometry observed for all of the anions in **1**–**8**. The distortion is consistent with being a response to the local electric field of the surrounding ions, thereby generating a dipole moment along the twofold axis of the anion (Scheme 1). This

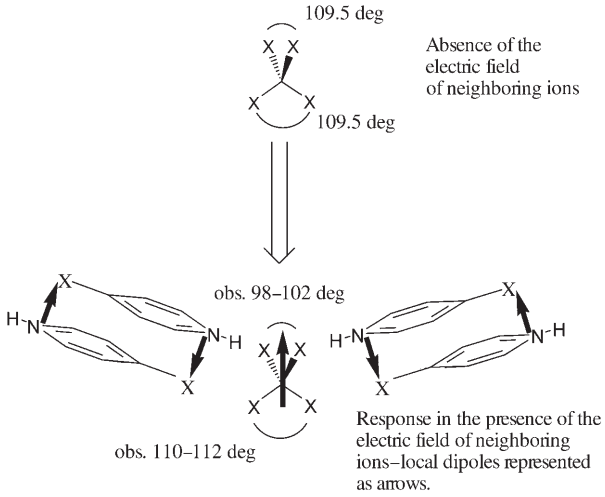

Scheme 1. Distortion of anion geometry in response to the electric field generated by neighboring ions. obs. = observed; dipole moments represented as arrows from + to −.

supposition is supported by theoretical calculations in which an optimization of the $[CoCl_4]^{2-}$ geometry was conducted in the presence of a simple model electric field that mimicked the orientation, if not the precise magnitude, of the field experienced by the ion in the crystal. The optimization resulted in compression of the Cl-Co-Cl angle closest to the positive end of the field and an increase in the associated pair of C–Cl bond lengths, with the reverse situation for the halide ligands closest to the negative end of the field.[21] This result is in qualitative agreement with the observed distortion of the $[CoCl_4]^{2-}$ ion in the crystal structures of **1** and **2**.

Comparison of intermolecular interaction geometries in chemically related compounds is often fraught with difficulty because of large differences between the crystal structures of the compounds, which can have a profound effect on the metrics of a given intermolecular interaction. The present study provides a remarkable opportunity to undertake such a comparison across eight isostructural compounds with systematic variation of both inorganic and organic halogen components for the recently identified, but potentially highly efficacious, class of M–X···X′–C halogen bonds. These interactions are highly directional, and X···X′ separations normalized to account for the change in size of the halogen atoms confirm that the interaction is shorter (stronger) for the heavier organic halogen species and demonstrate for the first time that this is also the case for the lighter inorganic halogen species. The trends in electrostatic potential at the halogen atoms, which becomes more positive for (C)Br > (C)Cl and more negative for (M)Cl > (M)Br > (M)I, are consistent with

these observations, thus clearly indicating that the electrostatic interaction between the halogen atoms is the dominant contribution in both directing and governing the strength of the M−X···X′−C halogen bonds. Given the abundance of the halogen atoms in molecular surfaces of both organic and inorganic systems, a clear understanding of the nature of M−X···X′−C halogen bonds provides an impetus for a wide range of applications to supramolecular construction of organic–inorganic hybrid materials and has the potential to yield applications in the control of conformations in metal complexes, molecular recognition, and substrate binding in catalysis.

Experimental Section

Crystal synthesis: All starting materials were purchased from Aldrich, Lancaster, or Avocado and used as received. Blue crystals of compounds **1**, **2**, **5**, and **6** were obtained in high yields following the evaporation of acidified solutions of $CoCl_2{\cdot}6H_2O$ or $CoBr_2$ combined with the appropriate 4-halopyridinium chloride, which had been previously dissolved in an excess of concentrated aqueous HX to prevent the formation of the mixed halide. Elemental analyses were in accord with expected values. Compounds **7** and **8** were obtained as green crystals by an analogous approach with $CoI_2{\cdot}2H_2O$ and acidification with concentrated aqueous HI, but only as the minor product, the major product being brown crystalline compounds $(4\text{-}XC_5NH_5)_2[CoI_4]{\cdot}I_2$, which will be discussed fully in a later publication. Crystals of mixed halide compounds **3** and **4** were obtained similarly but without acidification of the solutions. Small yields of compounds **3**, **4**, **7**, and **8** prohibited bulk analyses. Full details of the synthetic procedures can be found in the Supporting Information.

X-ray crystallography: X-ray data were collected at 150 K for **1**–**8** on a Bruker SMART 1000 diffractometer using $Mo_{K\alpha}$ X-rays. Data were corrected for absorption using empirical methods (SADABS) based upon symmetry-equivalent reflections combined with measurements at different azimuthal angles.[22] Crystal structures were solved and refined against all F^2 values using the SHELXTL suite of programs.[23] Non-hydrogen atoms were refined anisotropically and hydrogen atoms were placed in calculated positions refined using idealized geometries (riding model) and assigned fixed isotropic displacement parameters. For mixed halide compounds **3** and **4**, the Cl/Br ratio was allowed to refine independently for the two independent sites, thus leading to Cl/Br ratios of 0.562:0.438 and 0.221:0.779 for **3** and 0.570:0.430 and 0.241:0.759 for **4**, with physically reasonable displacement parameters for both sites. A summary of the data collection and structure refinements is provided in the Supporting Information. CCDC 279107–279114 contain the supplementary crystallographic data for this paper. These data can be obtained free of charge from the Cambridge Crystallographic Data Centre via www.ccdc.cam.ac.uk/data_request/cif.

Theoretical calculations: Electrostatic potential calculations for idealized $[CoX_4]^{2-}$ (X = Cl, Br, I) and $(4\text{-}X'pyH)^+$ (X′ = Cl, Br) ion geometries were conducted using the GAMESS-UK[24] package, which employs the B3LYP DFT functional.[25] The basis set used was the all-electron Ahlrichs DZ (double zeta) quality basis[26] on Co and Sadlej pVTZ (polarized valence triple-zeta) basis[27,28] for all other elements. Geometries for $[CoX_4]^{2-}$ ions were idealized using distances (taken from the crystal structure determinations) of 2.25 (Cl), 2.40 (Br), and 2.59 Å (I) and averaged X-Co-X angles from the pairs of crystal structures containing each anion. The halopyridinium ions used geometries constructed by averaging bond lengths and angles over all crystal structures and idealizing to a C_{2v} geometry, with C–X lengths of 1.72 (Cl) and 1.88 Å (Br). The distortion of the $[CoCl_4]^{2-}$ ion was simulated by undertaking a geometry optimization of the $[CoCl_4]^{2-}$ ion (tetrahedral starting geometry) using an Ahlrichs DZ quality basis[26] throughout, with a simple model electrical field generated by placing +1 and −1 charges at distances of 10 Å from the Co center displaced along the molecular twofold axis and by imposing C_{2v} symmetry on the anion.

Received: July 23, 2005
Published online: December 6, 2005

Keywords: crystal engineering · electrostatic interactions · halogen bonds · noncovalent interactions · organic–inorganic hybrid composites

[1] a) For example, of 325 709 crystal structures in version 5.26 of the Cambridge Structural Database[1b] (Nov. 2004), the number containing molecules with C−X bonds are 1595 (C–I), 7294 (C–Br), 27 064 (C–Cl), and 16 555 (C–F). The corresponding figures for compounds containing terminal M−X bonds (M = d- or f-block-metal centers) are 3361 (M–I), 4189 (M–Br), 26 892 (M–Cl), and 747 (M–F); b) F. H. Allen, *Acta Crystallogr. Sect. B* **2002**, *58*, 380.

[2] F. Zordan, L. Brammer, P. Sherwood, *J. Am. Chem. Soc.* **2005**, *127*, 5979.

[3] a) L. Brammer, G. Mínguez Espallargas, H. Adams, *CrystEngComm* **2003**, *5*, 343; b) F. Zordan, L. Brammer, *Acta Crystallogr. Sect. B* **2004**, *60*, 512; c) F. Zordan, S. L. Purver, H. Adams, L. Brammer, *CrystEngComm* **2005**, *7*, 350; d) see, also: R. D. Willett, F. Awwadi, R. Butcher, S. Haddad, B. Twamley, *Cryst. Growth Des.* **2003**, *3*, 301.

[4] a) G. Aullón, D. Bellamy, L. Brammer, E. A. Bruton, A. G. Orpen, *Chem. Commun.* **1998**, 653; b) L. Brammer, E. A. Bruton, P. Sherwood, *Cryst. Growth Des.* **2001**, *1*, 277.

[5] a) L. Brammer, J. K. Swearingen, E. A. Bruton, P. Sherwood, *Proc. Nat. Acad. Sci. USA* **2002**, *99*, 4956; b) J. C. Mareque Rivas, L. Brammer, *Inorg. Chem.* **1998**, *37*, 4756; c) G. R. Lewis, A. G. Orpen, *Chem. Commun.* **1998**, 1873; d) A. L. Gillon, G. R. Lewis, A. G. Orpen, S. Rotter, J. Starbuck, X.-M. Wang, Y. Rodríguez-Martín, C. Ruiz-Pérez, *J. Chem. Soc. Dalton Trans.* **2000**, 3897; e) A. Angeloni, A. G. Orpen, *Chem. Commun.* **2001**, 343; f) B. Dolling, A. L. Gillon, A. G. Orpen, J. Starbuck, X.-M. Wang, *Chem. Commun.* **2001**, 567; g) M. Felloni, P. Hubberstey, C. Wilson, M. Schröder, *CrystEngComm* **2004**, *6*, 87; h) V. Balamurugan, M. S. Hundal, R. Mukherjee, *Chem. Eur. J.* **2004**, *10*, 1683; i) C. J. Adams, P. C. Crawford, A. G. Orpen, T. J. Podesta, B. Salt, *Chem. Commun.* **2005**, 2457.

[6] P. Metrangolo, H. Neukirch, T. Pilati, G. Resnati, *Acc. Chem. Res.* **2005**, *38*, 386.

[7] J. P. M. Lommerse, A. J. Stone, R. Taylor, F. H. Allen, *J. Am. Chem. Soc.* **1996**, *118*, 3108.

[8] V. R. Pedireddi, D. S. Reddy, B. S. Goud, D. C. Craig, A. D. Rae, G. Desiraju, *J. Chem. Soc. Perkin Trans. 2* **1994**, 2353.

[9] a) M. Freytag, P. G. Jones, B. Ahrens, A. K. Fischer, *New J. Chem.* **1999**, *23*, 1137; b) E. Corradi, S. V. Meille, M. T. Messina, P. Metrangolo, G. Resnati, *Angew. Chem.* **2000**, *112*, 1852; *Angew. Chem. Int. Ed.* **2000**, *39*, 1782; c) P. Metrangolo, G. Resnati, *Chem. Eur. J.* **2001**, *7*, 2511; d) R. Bailey Walsh, C. W. Padgett, P. Metrangolo, G. Resnati, T. W. Hanks, W. T. Pennington, *Cryst. Growth Des.* **2001**, *1*, 165; e) P. K. Thallapally, G. R. Desiraju, M. Bagieu-Beucher, R. Masse, C. Bourgogne, J.-F. Nicoud, *Chem. Commun.* **2002**, 1052; f) A. Crihfield, J. Hartwell, D. Phelps, R. Bailey Walsh, W. T. Pennington, T. W. Hanks, *Cryst. Growth Des.* **2003**, *3*, 313; g) P. Metrangolo, T. Pilati, G. Resnati, A. Stevenazzi, *Chem. Commun.* **2004**, 1492; h) T. Caronna, R. Liantonio, T. A. Logothetis, P. Metrangolo, T. Pilati, G. Resnati, *J. Am. Chem. Soc.* **2004**, *126*, 4500.

[10] G. R. Desiraju, R. Parthasarathy, *J. Am. Chem. Soc.* **1989**, *111*, 8725.
[11] S. L. Price, A. J. Stone, J. Lucas, R. S. Rowland, A. E. Thornley, *J. Am. Chem. Soc.* **1994**, *116*, 4910.
[12] R. D. Bailey, M. R. Grabarczyk, T. W. Hanks, E. M. Newton, W. T. Pennington, *J. Chem. Soc. Perkin Trans. 2* **1997**, 2781.
[13] a) A. J. Blake, F. V. Devillanova, R. O. Gould, W.-S. Li, V. Lippolis, S. Parsons, C. Raddek, M. Schröder, *Chem. Soc. Rev.* **1998**, *27*, 195; b) P. H. Svensson, L. Kloo, *Chem. Rev.* **2003**, *103*, 1649.
[14] A. J. Bondi, *J. Chem. Phys.* **1964**, *68*, 441.
[15] $R_{XX'} = d(X\cdots X')/(r_X + r_{X'})$, where r_X and $r_{X'}$ are, respectively, the van der Waals radii[14] of halogen atoms X and X′ (following the definition of Lommerse et al.[7]); R_{HX} defined analogously for the H···X separation.
[16] It is anticipated that qualitative trend for halide anions should be the same as for an analogous series of perhalometallate ions, such as $[CoX_4]^{2-}$ ions.
[17] a) In $[CsI_3]$,[18a] $d(I{-}I) = 2.84$ Å; b) in $[CsBrI_2]$,[18b] $d(I{-}I) = 2.78$ Å; c) in (*N*-hexadecylpyridinium)$[BrI_2]$,[18c] $d(I{-}I) = 2.78$ Å; d) in (*N*-hexadecylpyridinium)$[ClI_2]$,[18c] $d(I{-}I) = 2.77$ Å.
[18] a) J. Runsink, S. Swen-Walstra, T. Migchelson, *Acta Crystallogr. Sect. B* **1972**, *28*, 1331; b) G. B. Carpenter, *Acta Crystallogr.* **1966**, *20*, 330; c) G. V. Shilov, O. N. Kazheva, O. A. D'yachenko, M. S. Chernov'yants, S. S. Simonyan, V. E. Gol'eva, A. I. Pyshchev, *Zh. Fiz. Khim.* **2002**, *76*, 1436.
[19] T. A. Logothetis, F. Meyer, P. Metrangolo, T. Pilati, G. Resnati, *New J. Chem.* **2004**, *28*, 760.
[20] We have shown recently that N–H···X hydrogen bonds form in preference to C–X′···X halogen bonds at the sites of greatest accumulation of negative charge on the halide when halide ions were compared with halometallate ions; see reference [3c].
[21] Calculated values for the $[CoCl_4]^{2-}$ ion in the model electrical field: Co-Cl(1) 2.421, Co-Cl(2) 2.338 Å; Cl(1)-Co-Cl(1′) 101.5, Cl(2)-Co-Cl(2′) 119.4°; where, Cl(1) and Cl(1′) are closest to the positive end of the field and Cl(2) and Cl(2′) are closest to the negative end. Slightly different values are obtained when using different basis sets, but the qualitative trend always matches the observed experimental distortion.
[22] a) G. M. Sheldrick, *SADABS:* Empirical absorption correction program, University of Göttingen, **1995**, based upon the method of Blessing;[22b] b) R. H. Blessing, *Acta Crystallogr. Sect. A* **1995**, *51*, 33.
[23] *SHELXTL* 5.1, Bruker Analytical X-Ray Instruments, Inc., **1998**.
[24] GAMESS-UK is a package of ab initio programs written by M. F. Guest, J. H. van Lenthe, J. Kendrick, K. Schoffel, P. Sherwood, with contributions from R. D. Amos, R. J. Buenker, H. J. J. van Dam, M. Dupuis, N. C. Handy, I. H. Hillier, P. J. Knowles, V. Bonacic-Koutecky, W. von Niessen, R. J. Harrison, A. P. Rendell, V. R. Saunders, A. J. Stone, A. H. de Vries; the package is derived from the original GAMESS code: M. Dupuis, D. Spangler, J. Wendoloski, NRCC Software Catalog, Vol. 1, Program No. QG01 (GAMESS), **1980**.
[25] a) P. J. Stephens, F. J. Devlin, C. F. Chabalowski, M. J. Frisch, *J. Phys. Chem.* **1994**, *98*, 11623, and references therein; b) *GAMESS-UK* uses the VWN 3 (RPA-type) parameterization; for details, see: R. H. Hertwig, W. Koch, *Chem. Phys. Lett.* **1997**, *268*, 345.
[26] The DZ Basis sets used were those incorporated into GAMESS-UK from A. Schafer, H. Horn, R. Ahlrichs, *J. Chem. Phys.* **1992**, *97*, 2571.
[27] All Basis sets and ECP data were obtained from the Extensible Computational Chemistry Environment Basis Set Database, Version 02/25/04, as developed and distributed by the Molecular Science Computing Facility, Environmental and Molecular Sciences Laboratory, which is part of the Pacific Northwest Laboratory (PO Box 999, Richland, Washington 99352, USA) and funded by the US Department of Energy. The Pacific Northwest Laboratory is a multiprogram laboratory operated by Battelle Memorial Institute for the US Department of Energy under contract DE-AC06-76RLO 1830. Contact David Feller or Karen Schuchardt for further information.
[28] A. J. Sadlej, *Theor. Chim. Acta* **1992**, *81*, 45, and references therein.

